ENTROPY GENERATION ANALYSIS FOR FORCED CONVECTION BOILING IN ABSORBER TUBES OF LINEAR FRESNEL REFLECTOR SOLAR THERMAL SYSTEM

by

Sanju THOMAS[a], Ajith G. KUMAR[a], Sudhansu S. SAHOO[b*], and Shinu M. VARGHESE[c]

[a] Department of Mechanical Engineering, COE, CUSAT, Ernakulum, India
[b] Department of Mechanical Engineering, CET, Ghatikia, Bhubaneswar, India
[c] Empereal-KGDS Renewable Energy Pvt. Ltd., Coimbatore, India

Original scientific paper
https://doi.org/10.2298/TSCI180331234T

A methodology has been presented related to entropy generation due to forced convection boiling in long absorber tubes used in linear Fresnel reflector solar thermal system. Variable heat flux has been applied on the tube which replicates the scenario for aforementioned tubes and local entropy generation has been obtained for various parameters. Mathematical modeling has been made separately for single-phase and two-phase regions in flow boiling conditions encountered in linear Fresnel reflector tubes. Entropy generation in two-phase region has been formulated using homogeneous equilibrium model. The entropy generation at varying mass flux and heat flux cases are calculated. The entropy generation due to heat transfer is found to be more than that of pressure drop. Still, entropy generation due to pressure drop in two-phase region plays a major role of increasing nature of it. Present approach will help researchers and industry to optimize the solar thermal systems where flow related phase change occurs and measures can be taken accordingly to increase energy efficiency of those systems.

Key words: *entropy generation, linear Fresnel reflector solar thermal, variable heat flux, homogeneous equilibrium model*

Introduction

The essential operational problem with solar collectors or receivers is the collection and delivery of solar energy to process plant or for other utilities with minimum losses. Different modes of performance can be adopted for investigation of the ideal operating conditions of solar collectors. Collector tube needs optimized conditions to be operated for reduction of total cost and better efficiency due to its higher cost in any solar thermal system. One important way to get performance of solar collectors can be investigated from the entropy generation point of view (Second law analysis of thermodynamics), which is an effective method to correlate, not to alter the energy analysis (First law analysis of thermodynamics).

In recent years, few authors have studied different features of solar collector system using exergetic approaches. Detailed exergy analysis of various kinds of solar thermal collectors and processes are reviewed and mentioned [1]. Energy and exergy analysis of flat plate solar collectors have been carried out by Jafarkazemi and Ahmadifard [2] and Ge *at al*. [3].

* Corresponding author, e-mail: sahoo.sudhansu@gmail.com

The exergetic analysis of finned double-pass solar collectors has been evaluated by Fudholi *et al.* [4]. Al-Sulaiman [5] presented a detailed exergy analysis of selected thermal power systems driven by parabolic trough solar collectors. The energy and exergy analysis of parabolic trough solar collectors are investigated by Hou *et al.* [6]. Padilla *et al.*[7] presented an exergy analysis to study the effects of operational and environmental parameters on the performance of parabolic trough collectors. Nixon *et al.* [8] proposed novel solar thermal collector concepts derived from the linear Fresnel reflector (LFR). The authors developed a multi-criteria decision-making methodology, which included the exergy as a tool. Experimental investigations of energy and exergy analysis of paraboloid dish system are carried out by Madadi *et al.* [9]. Thermal model for optimum design of a 3-D compound parabolic concentrator considering the maximization of exergy delivers are found in literature by Nishi and Qi [10]. Numerical study of 3-D diffusive natural-convection in an inclined solar distiller has been established [11]. Momentum and heat transfer rates as well as entropy generation have been numerically investigated for fully developed forced convection, laminar flow in a micro-pipe [12].

From literature review, we focus the fact that, quite some attempts have been made in the past to assess entropy generation in low length solar thermal systems like solar air heater, flat collectors, parabolic trough collectors. Entropy generation analysis of convective flow in the tubes used in those collector systems are rarely mentioned. Those mentioned in literatures related to flow analysis are based on single-phase flow, which mostly occur in flat plate heaters or air heaters. In all those system, fluid does not undergo change of phase, so studies mainly highlight the estimation of entropy generation in single-phase flow only. Even on two-phase flow, entropy generation analysis were mentioned for small length components like evaporators, condensers [13] but the heat flux has been considered constant along the length of the tube. To the best of author's knowledge, entropy generation analysis using Second law of thermodynamics had rarely been reported as for long tubes with integrated single-phase flow and two-phase flow. Again, almost no work has been reported as for as variable heat fluxes for the systems to calculate entropy generation is concerned.

Considering the previous literature gaps, a methodology has been presented in this present work which takes care of longer tubes (384 m), variable heat flux, single as well as two-phase region for finding local entropy generation in tubes of LFR systems. Energy analysis which is required for entropy analysis has been formulated too. Net heat flux which useful for the system is variable in nature along the flow direction is considered. Entropy generation in two-phase region has been formulated using verified homogeneous flow model [14, 15]. The outcome of this entropy generation analysis will help researchers and industry to optimize the solar thermal systems where flow related phase change occurs and measures can be taken accordingly to increase energy efficiency of those systems.

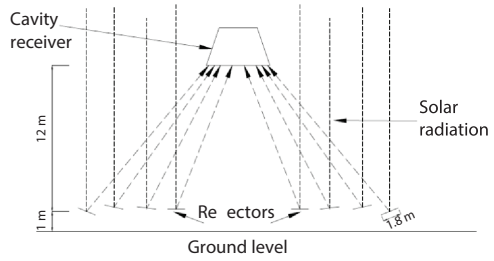

Figure 1. The LFR solar thermal system used in present work

The LFR system and set-up description

The LFR solar thermal system consists of parallel rows of linearly coupled reflector units or plane mirror strips and a linear, fixed cavity receiver at appropriate height above the reflectors, fig. 1. Cavity receiver, usually trapezoidal shaped, contains single or multiple tubes which are subjected to reflected solar rays from the reflectors, fig. 2. The inside of the cavity, external to the tubes, contains air which is not in contact

with the ambient. The water running through the tubes inside the cavity absorbs heat from the reflected rays from the LFR field, passing through the bottom glass cover of the trapezoidal cavity. Heat transfer fluids, usually, water enters the tube at high pressure and sub-cooled temperature which gets heated due to incident reflected heat flux from reflective mirrors as shown in fig 1.

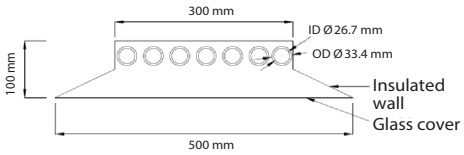

Figure 2. Trapezoidal cavity receiver in considered LFR solar thermal system

Under concentrated solar flux, tube wall increases and water temperature increases till it reaches the saturation temperature corresponding to the system pressure. The region beginning from the entry to the length at which the mean fluid temperature reaches saturation temperature is termed as single-phase flow region. Beyond this length boiling takes place and the steam dryness fraction increases and this region is termed as two-phase region. This whole process is nothing but forced convection boiling or convective flow boiling.

Table 1. The LFR specifications in the present study

Receiver bottom width	500 mm
Receiver top width	300 mm
Receiver side length	141 mm
Receiver depth	100 mm
No of tubes in the receiver cavity	08
Absorber tube inner diameter	26.7 mm
Outer diameter of the absorber tube	33.4 mm
Length of the absorber tube	384 m
Numbers of mirrors	08
Width of mirror	1.8m
Positions of mirrors from the ground	01 m
Positions of receiver from the ground	13 m
Optical efficiency of the LFR system	80%

The LFR system under discussion consists of a trapezoidal shaped cavity receiver, fig. 2, filled with air and houses eight parallel, uninterrupted and long absorber tubes for direct steam generation. Absorber tubes are made of SS304 having dimensions as mentioned in tab. 1. This cavity receiver with eight tubes in it receives reflected radiation from eight parallel mirrors/reflectors of 1.8 m width each along the entire length of reflection. The reflector arrangements are shown in fig. 2 and specifications are given in tab. 1. The trapezoidal cavity receiver consists of four sides. The bottom cover made of glass receives concentrated solar rays and minimize convective heat loss from the cavity due to wind effects below it. The rest three sides are insulated to reduced conduction heat loss.

Mathematical modelling

The schematic diagram of the 1-D tube flow model is shown in fig. 3. At distance z from the inlet, flow parameters can be seen in the figure. As discussed earlier, the variable net heat flux is subjected to absorber tube.

Although, the concentrated incident heat flux is the same throughout the length of the tube, heat losses (which are dependent upon the temperature of the outer tube wall) vary along the length.

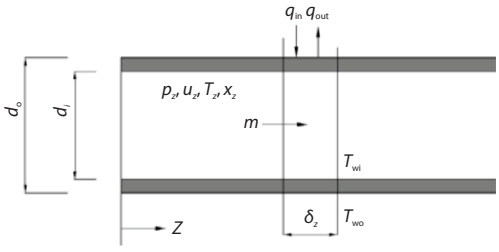

Figure 3. Tube flow model

Therefore, the analysis of the flow inside the absorber tube should take into account the effect of the heat losses in the axial direction and that is why variable net heat flux enters the fluid through the tube wall along the length. However, computation of heat losses from the sur-

Table 2. Overall heat loss coefficient w.r.t tube wall temperature

Outer wall temperature of the absorber tube [K]	Overall heat loss coefficient [$Wm^{-2}K^{-1}$]
310	2.2
350	2.8
390	3.2
430	3.7
470	4.2
510	4.8
550	5.5
590	6.1

face of the absorber tube in LFR cavity is not straightforward. To obtain the aforementioned heat losses, the heat transfer coefficient as a function of temperature is needed. This coefficient, tab. 2, is obtained by using the correlations mentioned in literature [14, 15].

Single-phase region

In this region, the bulk fluid temperature remains below saturation fluid temperature. In a flow passage of cross-section, A_{cs} and the heat transferring surface perimeter of πd_0, the bulk fluid properties of the fluid having mass rate, $\dot{m}$ are T_f, p, i, s, and ρ. In general the heat transfer phenomenon is characterized by a finite frictional pressure gradient, $(-dp/dx) > 0$, when heat is transferred to the fluid at a heat rate q' [Wm^{-1}] by finite wall-bulk fluid temperature difference ΔT_m. Considering a slice of thickness dz as a small system in the flow domain, the rate of entropy generation for one inlet and one exit control volume:

$$dS_{\text{gen}} = \dot{m}ds - \frac{q'_{\text{net}}dz}{(T_{\text{f}} + \Delta T_m)} \tag{1}$$

The First law/energy equation for the system:

$$\dot{m}di = q'_{\text{net}}dz \tag{2}$$

where

$$q'_{\text{net}} = \left[q''_{\text{in}} - U_L\left(T_{\text{wo}} - T_{\text{a}}\right)\right]\left(\pi d_o\right) \tag{3}$$

Heat influx on the tube wall is found out using following equation:

$$q''_{\text{in}} = \frac{\left[DNI\,\rho_g\left(\sum A_r\cos\theta_n\right)\gamma(\tau\alpha)\right]}{\left[n_t\pi d_o L\right]} \tag{4}$$

where DNI is the direct normal irradiation on the reflector surface at a particular time and day of the year. The $\sum A_{\text{r}}\cos\theta_{\text{n}}$ is the effective reflector area that faces towards the receiver which is situated at the top. The ρ_{g}, γ, $\tau\alpha$ are the the mirror reflectivity, mirror field solidity factor and absorptivity-transmissivity of the glass cover, respectively.

The U_L is the overall heat loss coefficient, which is dependent upon outer wall temperature of the tube [14, 15].

The Second law to the same system:

$$T_{\text{f}}ds = di - \frac{dp}{\rho} \tag{5}$$

Substituting eqs. (2), (3), and (5) in eq. (1) and simplifying:

$$dS'_{\text{gen}} = \frac{dS_{\text{gen}}}{dz} = \frac{\left[q''_{\text{in}} - U_L\left(T_{\text{wo}} - T_{\text{a}}\right)\right]\left(\pi d_o\right)\Delta T_m}{T_{\text{f}}^2\left(1 + \dfrac{\Delta T_m}{T_{\text{f}}}\right)} + \frac{\dot{m}}{\rho T_{\text{f}}}\left(-\frac{dp}{dz}\right) \tag{6}$$

The first term in eq. (6) can be denoted as ($dS'_{\text{gen},\Delta T}$) represents the entropy generation due to heat transfer caused as a result of the wall-fluid temperature difference and the second term denoted as ($dS'_{\text{gen},\Delta p}$) is the entropy generation caused by fluid friction.

The T_{wo} and T_f can be found out by simplifying eq. (2) and eq. (3):

$$T_{wo} = \frac{\left[T_{in} + \pi d_o dz\left(q''_{in} + U_L T_a\right)\left(R_{th} + \frac{1}{2\dot{m}c}\right)\right]}{\left[1 + U_L\left(\pi d_o dz\right)\left(R_{th} + \frac{1}{2\dot{m}c}\right)\right]} \tag{7}$$

$$T_f = T_{in} + \left[q''_{in} - U_L\left(T_{wo} - T_a\right)\right]\frac{\pi d_o dz}{2\dot{m}c} \tag{8}$$

Thermal resistance, R_{th} can be written:

$$\sum R_{th} = \frac{1}{2\pi k_s dz}\ln\left(\frac{d_o}{d_i}\right) + \frac{1}{h_f \pi d_i dz} \tag{9}$$

Dittus-Boelter equation can be applied to obtain local heat transfer coefficient, h_f.

Similarly, pressure drop across the channel length dp can be obtained using famous Darcy-Weisbach formula.

Convective heat transfer processes are generally characterized by two types of losses, namely losses due to heat transfer across a finite temperature difference and losses due to fluid friction across the flow direction [16, 17]. Both types of losses are the display of thermodynamic irreversibility.

Two-phase region

In this region where the bulk fluid temperature remains constant till dry state reaches. Various approaches are found in the literature related two-phase flow modelling. The relatively simpler homogeneous equilibrium model (HEM) which assumes a slip ratio (ratio of gas velocity to liquid velocity) equal to one and assumes fluid properties as averaged properties of gas and liquid has been adopted here. As the ratio of length to diameter of the tube is more than 100, this HEM approach is best suited for the present condition [14, 15].

Homogeneous quantity of all fluid properties in this region:

– enthalpy

$$i_{hom} = i_l + x(i_g - i_l) \tag{10}$$

– entropy

$$s_{hom} = s_l + x(s_g - s_l) \tag{11}$$

– density

$$\rho_{hom} = \left(\frac{x}{\rho_g} + \frac{1-x}{\rho_l}\right)^{-1} \tag{12}$$

– void fraction

$$\alpha = \left[1 + \left(\frac{1-x}{x}\right)\frac{\rho_g}{\rho_l}\right]^{-1} \tag{13}$$

In a flow passage of cross-section, A_{cs} and the heat transferring surface perimeter of (πd_o), the bulk fluid properties of the fluid having mass rate, $\dot{m}$ are T_{sat}, p, i_{hom}, s_{hom}, and ρ_{hom}. Like single-phase flow, the heat transfer arrangement in two-phase region is also characterized by a finite frictional pressure gradient, $(-dp/dx) > 0$, when heat is transferred to the fluid at a rate q' [Wm^{-1}] by finite wall-bulk fluid temperature difference ΔT_m, which remains more or less

constant in this region. Considering a slice of thickness *dz* as a small system, the rate of entropy generation for one inlet and one exit control volume:

$$dS_{\text{gen}} = \dot{m} ds_{\text{hom}} - \frac{q'_{\text{net}} dz}{(T_{\text{sat}} + \Delta T_m)} \tag{14}$$

The First law/energy equation for the system:

$$\dot{m} d_{i\text{hom}} = q'_{\text{net}} dz \tag{15}$$

The Second law applied to the same system:

$$T_{\text{sat}} ds_{\text{hom}} = d_{i\text{hom}} - \frac{dp_{\text{tp}}}{\rho_{\text{hom}}} \tag{16}$$

we get:

$$dS'_{\text{gen}} = \frac{dS_{\text{gen}}}{dz} = \frac{\left[q''_{\text{in}} - U_L \left(T_{\text{wo}} - T_{\text{a}}\right)\right]\left(\pi d_o\right)\Delta T_m}{T_{\text{sat}}^2 \left(1 + \dfrac{\Delta T_m}{T_{\text{sat},z}}\right)} + \frac{\dot{m}}{\rho_{\text{hom}} T_{\text{sat},z}} \left(-\frac{dp}{dz}\right)_{\text{tp}} \tag{17}$$

The first term from eq. (17) can be denoted as ($dS'_{\text{gen},\Delta T}$) which represents the entropy generation due to heat transfer across the wall-fluid temperature difference and the second term denoted as ($dS'_{\text{gen},\Delta p}$) is the entropy generation caused by fluid friction.

For getting ρ_{hom}, steam quality need to be calculated, which can be found out by simplifying eq. (14) and is expressed:

$$x_{\text{f}} = x_{\text{in}} + \left[q''_{\text{in}} - U_L (T_{\text{wo}} - T_{\text{a}})\right] \frac{\pi d_o dz}{2 \dot{m} i_{\text{lg}}} \tag{18}$$

Friedel correlation [18] can be used to find the pressure loss in two-phase region which is required for the ($dS'_{\text{gen},\Delta p}$).

Results and discussion

For entropy generation calculation based on the modeling in the previous section, various parameters are varied such as Irradiation or DNI varied from 700-900 W/m^2. Similarly mass flux has been varied from 200-400 kg/sm^2. Inlet pressure and temperature are kept at 45 bar and 308 K for all calculations. Axial temperature variation of fluid in the tube based on the variable heat flux corresponding direct normal irradiation of the value 900 W/m^2 is shown in fig. 4.

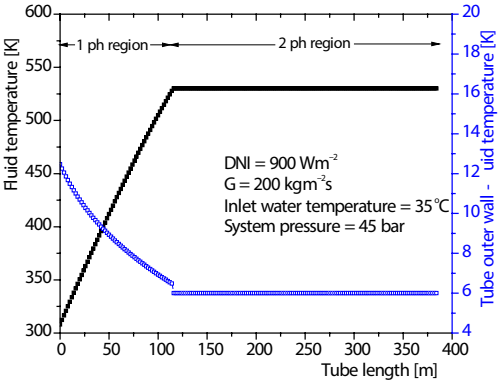

Figure 4. Axial variation of bulk fluid temperature and difference between tube wall and fluid temperature

It also denotes difference between outer wall and fluid temperature. It can be seen that, temperature of fluid goes on increasing up to certain length (119 m) and then after, the fluid temperature remains almost constant. It implies that there are two regions exist in the flow field. Hence, after 119 m length, the region is considered as two-phase region which happens due to forced convection boiling. It can be seen also that the variation between tube wall and fluid varies from 6-13 K across the flow direction.

Figure 5 denotes the void fraction variation with dryness fraction or steam quality variation in two-phase region. It is seen that the void fraction increases quickly up to 0.2 steam quality and the rate of increase of void fraction decreases after that.

Figure 6 describes the variation of entropy generation with heat transfer and pressure drop along the length of the tube. Equations (6) and (17) are used to find the entropy generation along the length of tube. The values may be said as local entropy generation as well. It is visible that, the entropy generation decreases in the single-phase region. Although pressure drop rises but net heat transfer decreases in this region. It can be stated that entropy generation is more dependent on heat transfer rather than pressure drop in single-phase region. The trend is found opposite in the two-phase region. In two-phase region, heat transfer is almost constant but two-phase pressure drop rises rapidly even more than single-phase region [16]. Again, it can be seen that entropy generation increases slightly in the two-phase region. The entropy generation due to heat transfer is small in the two-phase region.

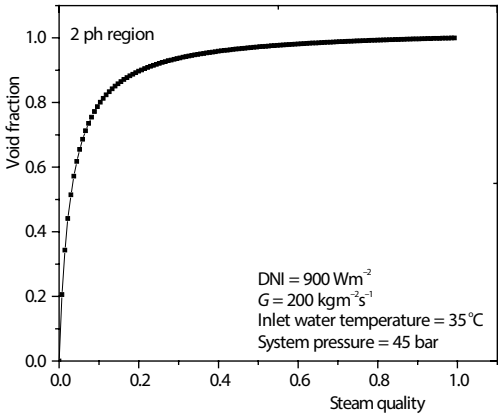

Figure 5. Void fraction variation w.r.t steam quality in two-phase region

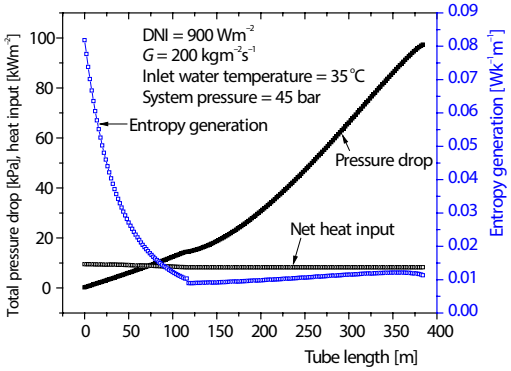

Figure 6. Axial variation of entropy generation and pressure drop

Entropy generation due to pressure drop is the important reason for increasing trend in the two-phase region. After certain steam quality, the entropy generation due to heat transfer increases again. Influence of heat input due to irradiation at varying mass flux conditions on entropy generation in the system (whole absorber tube length) is depicted in fig. 7. Sum of the length wise local entropy generation, based on eqs. (6) and (17), is considered as global entropy generation or entropy generation in the system. It can be clearly seen that with more heat addition the system, the entropy generation due to heat transfer increases although the increase of entropy generation due to pressure drop is not significant.

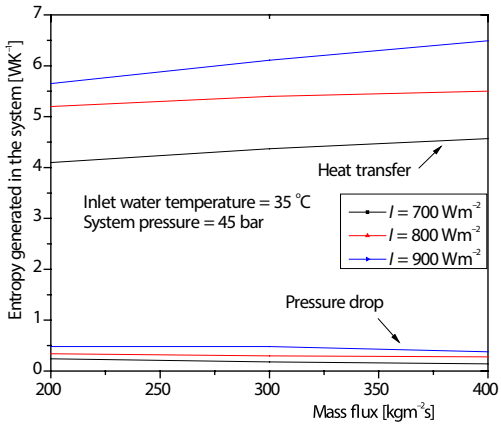

Figure 7. Influence of heat addition on entropy generation at varying mass flux conditions

Figure 8 shows the irreversibility associated with entropy generation (T_oS_{gen}) at varying mass flux conditions. Atmospheric temperature, T_o is considered as 303 K for the calcula-

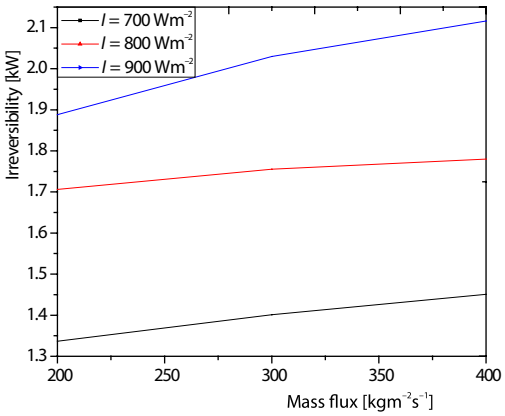

Figure 8. Irreversibility due to entropy generation at varying mass flux conditions

tions. It can be seen that with increase in mass flux, the entropy generation increase, but the slop of rise decreases in higher mass flux cases. Similarly, with more heat input to the system due more irradiation cases, the entropy generation increases appreciably.

Conclusion

Entropy generation rate has been the attraction of research, since it provides information on the thermodynamic irreversibility associated with the thermal systems particularly solar thermal systems. Here, an attempt was made to analyse the entropy generation during flow boiling phenomena that occurs in LFR absorber tubes. Mathematical modelling has been made separately for single-phase and two-phase regions in flow boiling conditions. Homogeneous model which is little simpler has been adopted to two-phase model which was required to find entropy generation for two-phase region. The entropy generation at varying mass flux and heat flux were mentioned in this work. The entropy generation due to heat transfer is found to be more than due to that due to pressure drop. Still, entropy generation due to pressure drop in two-phase region plays a major role of increasing nature of it. As minimization of entropy generation leads to better performance, so work on reducing pressure drops is needed. Simultaneously, heat transfer rates from wall to fluid need to be enhanced for better performance of LFR tubes. Entropy minimization analysis is the scope of future work. Further work can be carried out such analysis with different two-phase flow models like drift flux models, separated flow models.

Nomenclature

A_{cs} – tube cross-section, [m^2]
A_r – reflector/mirror area, [m^2]
c – specific heat, [Jkg^{-1}K^{-1})
d – nominal diameter, [m]
d_i – inner diameter, [m]
d_o – outer diameter of the pipe, [m]
ds – entropy change, [Jkg^{-1}K^{-1}]
dz – elementary length, [m]
h – heat transfer coefficient, [Wm^{-2}K^{-1}]
I – direct normal irradiation, [Wm^{-2}]
i – enthalpy, [Jkg^{-1}]
i_{lg} – latent heat of vaporization, [Jkg^{-1}]
k – thermal conductivity, [Wm^{-1}K^{-1}]
L – length of the absorber tube, [m]
$\dot{m}$ – mass-flow rate, [kgs^{-1}]
n_t – number of tubes
p – pressure, [Nm^{-2}]
q' – heat rate, [Wm^{-1}]
q'' – heat flux, [Wm^{-2}]
R_{th} – thermal resistance
T – temperature, [K]
U_L – overall heat loss coefficient, [Wm^{-2}K^{-1}]
x – steam quality

Greek letters

γ – solidity factor
θ – angle made by mirrors with horizontal axis, [degree]
ρ – reflectivity, density, [kgm^{-3}]
$\tau\alpha$ – transmissivity-absorptivity coefficient

Subscripts

a – air
f – fluid
g – gas
gen – generation
hom – homogeneous
in – input, inlet
l – liquid
lg – latent
net – input-loss
o – outer periphery

out – output
r – radiation, reflector
s – solid, steel material
sat – saturation
tp – two-phase region
wo – wall out
wi – wall in

References

[1] Kalogirou, S. A., *et al*., Exergy Analysis on Solar Thermal Systems: A Better Understanding of their Sustainability, *Renewable Energy*, *85* (2016), Jan., pp. 1328-1333
[2] Jafarkazemi, F., Ahmadifard, E., Energetic and Exergetic Evaluation of Flat Plate Solar Collectors, *Renewable Energy*, *56* (2013), Aug., pp. 55-63
[3] Ge, Z., *et al*., Exergy Analysis of Flat Plate Solar Collectors, *Entropy*, *16* (2014), 5, pp. 2549-2567
[4] Fudholi, A., *et al*., Energy Analysis and Improvement Potential of Finned Double Tube-Pass Collector, *Energy Conversion and Management*, *75* (2013), Nov., pp. 234-240
[5] Al-Sulaiman, F. A., Exergy Analysis of Parabolic trough Solar Collectors Integrated with Combined Steam and Organic Rankine Cycles, *Energy Conversion and Management*, *77* (2014), Jan., pp. 441-449
[6] Hou, H., *et al.*, Exergy Analysis of Parabolic trough Solar Collector, *Taiyangneng Xuebao/Acta Energiae Solaris Sin*, *35* (2014), pp. 1022-1028
[7] Padilla, R. V., *et al*., Exergy Analysis of Parabolic trough Solar Receiver, *Applied Thermal Engineering*, *67* (2014), 1-2, pp. 579-586
[8] Nixon, J. D., *et al*., Design of a Novel Solar Thermal Collector Using a Multi-Criteria Decision-Making Methodology, *Journal of Cleaner Production*, *59* (2013), Nov., pp. 150-159
[9] Madadi, V., *et al.*, First and Second Thermodynamic Law Analyses Applied to a Solar Dish Collector, *Journal of Non-Equilibrium Thermodynamics*, *39* (2014), 4, pp. 183-197
[10] Nishi, Y., Qi, X., Exergy Analysis on Solar Heat Collection of 3-D Compound Parabolic Concentrator, *International Journal of Exergy*, *13* (2013), 2, pp. 260-280
[11] Ghachem, K., *et al*., Numerical Study of Heat and Mass Transfer Optimization in a 3-D Inclined Solar Distiller, *Thermal Science*, *21* (2017), 6A, pp. 2469-2480
[12] Alper Ozalp, A., Entropy Analysis of Laminar-Forced Convection in a Pipe with Wall Roughness, *International Journal of Exergy*, *6* (2009), 2, pp. 249-275
[13] Revellin, R., Bonjour, J., Entropy Generation during Flow Boiling of Pure Refrigerant and Refrigeration Oil Mixture, *International Journal of Refrigeration*, *34* (2011), 4, pp. 1040-1047
[14] Sahoo, S. S., *et al*., Steady Sate Hydrothermal Analysis of Absorber Tubes Used in Linear Fresnel Reflector Solar Thermal System, *Solar Energy*, *87* (2013), Jan., pp. 84-95
[15] Sahoo, S. S., *et al.*, Thermal Hydraulic Simulation of Absorber Tubes in Linear Fresnel Reflector Solar Thermal System Using RELAP, *Renewable Energy*, *86* (2016), Feb., pp. 507-516
[16] Bejan, A., *Convective Heat Transfer*, 2nd ed., John Wiley and Sons, New York, USA, 1999
[17] Bejan, A., Fundamentals of Exergy Analysis, Entropy Generation Minimization, and the Generation of Flow Architecture, *International Journal of Energy Research*, *26* (2002), 7, pp. 0-48
[18] Friedel, L., Improved Friction Drop Correlations for Horizontal and Vertical Two-Phase Pipe Flow, European Two-Phase Flow Group Meeting, Paper E2, Ispra, Italy, 1979

Paper submitted: March 31, 2018
Paper revised: June 30, 2018
Paper accepted: August 1, 2018